Optical visible wavelength region selective reflector design for photovoltaic cells using photonic crystal

Veysel KORKMAZ[1], **Ali ÇETİN**[2,*]
[1]Information and Communication Technologies Authority, Ankara, Turkey
[2]Department of Physics, Faculty of Arts and Sciences, Eskişehir Osmangazi University, Eskişehir, Turkey

Abstract: In this study, we have proposed an optical broadband angular reflector having a band selective feature and high reflectivity rate for photovoltaic implementations by using a photonic crystal structure made of two different dielectric layers. This paper presents new and useful information about a reflector that was designed by using a periodic structure composed of two Si based layers for the visible range in the solar spectrum region. The system has been adjusted in such a way that it could cover a wide wavelength area between the photonic band gaps at nearly $\lambda \approx 300$–800 nm. We have tested the proposed reflector against different angles of incidence of the light. The reflectivity spectra of the optical structure have been calculated.

Key words: Solar cell, photonic crystals, broadband reflector, photonic band gap

1. Introduction

Photonic crystals (PCs) are structures for which the dielectric constant varies periodically, and through this specification, they can be used to prevent the propagation of electromagnetic waves in certain directions and in certain frequency gaps.

The frequency gap is called the photonic band gap, in which PCs have shown powerful reflections in this study. The motion and confinement of light in the desired area can be controlled in PCs by using different materials and geometrical parameters. By this means, light could be directed to a desired area of the device. Due to this convenient feature, the use of PCs in photovoltaic applications has risen in recent years [1–7].

In today's world, the most productive solar cells are manufactured from silicon. The spectral range for silicon solar cells is between $\lambda \sim 300$ nm and $\lambda \sim 1100$ nm, as shown in Figure 1 [8]. Silicon, which has a rather wide visible range, provides a great advantage in solar cell applications. The typical range of optical structures corresponding to the spectral area has the range of several hundreds of nanometers. Therefore, although it has a wide wavelength gap, it is quite difficult to get the effects desired for the visible spectrum in the solar cell. Within the scope of supplying the production, in order to concentrate the angle of incidence of the light, it seems obligatory to use additional special designs with high manufacturing costs and to use mirrors.

On the other hand, by using structures particularly designed with PCs, they are likely to emit the radiation in the wavelength gap best absorbed only by a solar battery. In order to carry out such activity, there is no need for an additional mechanism as in other systems.

While selecting the regions where the sunshine reaches its peak, the light is directed with proper designs
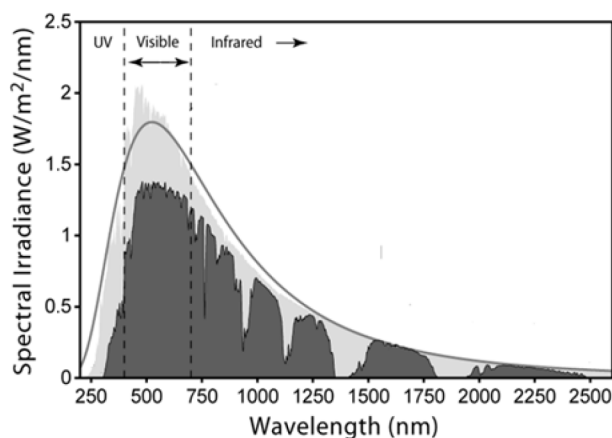
---

*Correspondence: acetin@ogu.edu.tr

Figure 1. Solar radiation spectrum. The visible part of the spectrum is located between 380 nm and 750 nm wavelength.

at the same time and it is trapped in the solar cell and helps provide more absorption. The concepts of providing and accumulating the rays can be formed in order to focus and keep the sunshine and sun radiation in the cell with a PC reflector integrated to a solar cell without using external sun reflectors and sun mirrors. The focusing of the trapped light in the solar cells increases the productivity and decreases the thickness of the solar cell. Thus, several light trapping concepts aim to increase the way the light travels and penetrates into the solar cell [9–21].

Wavelength selective device modeling has great importance for photovoltaic applications. This study aims to perform a numerical investigation of PCs. Numerical studies on choosing the appropriate material and determining the parameters of material have significant contributions for the manufacturing of highly productive devices. The reflectivity spectra of this photonic structure have been simulated by using a periodic photonic crystal.

In this work, a perfect reflector is designed by using a periodic structure composed of two Si based layers for the visible range in the solar spectrum region. Similarly, besides focusing the light in the solar cell concept, the device acts as a filter, allowing the desired spectrum band gap to pass. Since light is adjustable for different angles of incidence and as its fabrication is simple and cheap, it can be used comfortably in a number of photovoltaic (PV) cell applications.

2. Theory and method

A 1D PC multilayer structure is shown in Figure 2, which has been made of two different periodic dielectric layers. The layers having two different refractive indexes are labeled as A and B, whose thicknesses are d_1 and d_2, respectively. The system can be defined as air/(AB)^N/substrate. In a multilayer periodic structure made of PC pairs with the number N, the reflectivity rate for an electromagnetic wave with the angle of incidence θ to the boundary of air layer 1 is calculated by using Abeles theory [22].

By applying Maxwell limit conditions at an interface whose refractive index is different, the mathematical equations are solved and in particular the characteristic matrix $M(\Lambda)$ of the system for a single period is found. This matrix is independent of the polarization of the incident wave. In solving the system equations and in reducing the equation numbers, the method to provide an optimal solution is the transfer matrix method.

For the transverse electric (TE) polarization, the characteristic matrix $M(\Lambda)$ belonging to a period [22,23]
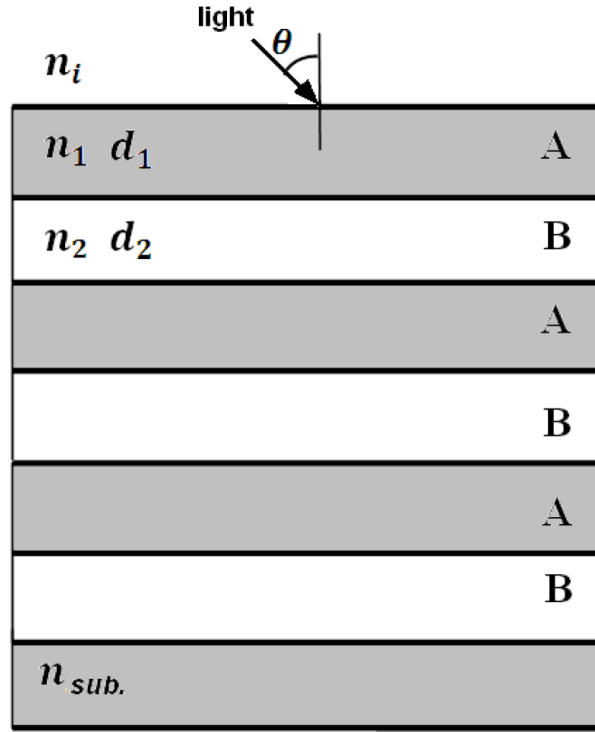
Figure 2. Schematic representation of a multilayered photonic crystal structure consisting of alternate layers.

is:

$$M(\Lambda) = \begin{bmatrix} M_{11} & M_{12} \\ M_{21} & M_{22} \end{bmatrix} = \prod_{i=1}^{K} \begin{bmatrix} \cos\beta_i & -\frac{1}{jp_i}\sin\beta_i \\ -jp_i\sin\beta_i & \cos\beta_i \end{bmatrix}. \tag{1}$$

It is assumed that there are two layers with different refractive indexes; therefore, K = 2. In Eq. (1), $\Lambda = d_1 + d_1$ is the period and $\beta_i = \frac{2\pi}{\lambda} n_i d_i \cos\theta_i$, $P_i = n_i \cos\beta_i$. β_i is the angle of incidence of the light to the layer with a refractive index n_i. n_1 and n_2 are the refractive indexes of each layer.

For the transverse magnetic (TM) polarization, calculations can be made by replacing $P_i = \frac{\cos\theta_i}{n_i}$ (i=1, 2). Matrix elements are obtained by using Eq. (1).

$$M_{11} = \cos\beta_1\cos\beta_2 - \frac{p_2}{p_1}\sin\beta_1\sin\beta_2 \tag{2a}$$

$$M_{12} = -j\left(\frac{1}{p_2}\cos\beta_1\sin\beta_2 + \frac{1}{p_1}\sin\beta_1\cos\beta_2\right) \tag{2b}$$

$$M_{21} = -j\left(p_1\sin\beta_1\cos\beta_2 + p_2\cos\beta_1\sin\beta_2\right) \tag{2c}$$

$$M_{22} = \cos\beta_1\cos\beta_2 - \frac{p_1}{p_2}\sin\beta_1\sin\beta_2 \tag{2d}$$

A multilayer structure with the periodic number N of the total characteristic matrix can be indicated as:

$$M = M(N\Lambda) = = [M(\Lambda)]^N. \tag{3}$$

The total characteristic matrix can be written as:

$$M = \begin{bmatrix} m_{11} & m_{12} \\ m_{21} & m_{22} \end{bmatrix} = \begin{bmatrix} M_{11} & M_{12} \\ M_{21} & M_{22} \end{bmatrix}^N, \tag{4}$$

where the matrix elements of M are obtained from the elements of the matrix with a single period provided that:

$$m_{11} = M_{11}U_{N-1}(a) - U_{N-2}(a), \tag{5a}$$

$$m_{12} = M_{12}U_{N-1}(a), \tag{5b}$$

$$m_{21} = M_{21}U_{N-1}(a), \tag{5c}$$

$$m_{22} = M_{22}U_{N-1}(a) - U_{N-2}(a). \tag{5d}$$

In the above equations U_N is a Chebyshev polynomial and expressed as:

$$U_N(a) = \frac{\sin\left[(N+1)\cos^- a\right]}{\sqrt{1-a^2}}, \tag{5e}$$

where a is a half trace of a single periodic matrix and determined as:

$$a = \cos\beta_1\cos\beta_2 - \frac{1}{2}\left(\frac{p_1}{p_2} + \frac{p_2}{p_1}\right)\sin\beta_1\sin\beta_2, \tag{6}$$

with $a = \frac{1}{2}(M_{11} + M_{22})$.

By obtaining the matrix elements from the equation, the reflections rates are written [22,23] as:

$$r = \frac{(m_{11} + m_{12}p_s)\,p_0 - (m_{21} + m_{22}p_s)}{(m_{11} + m_{12}p_s)\,p_0 + (m_{21} + m_{22}p_s)}, \tag{7}$$

where $p_0 = n_0\cos\theta_0$, $p_s = n_s\cos\theta_s$, n_0 is the refractive index of air, n_s is the refractive index of the substrate layer, and θ is the angle of incidence from the left side of the boundary of air layer 1.

From the above equations, reflectance can be expressed as:

$$R = |r^2| = f(\lambda, \theta). \tag{8}$$

3. Results

The periodic PC structure is considered with a sequence of air/(AB)^N/substrate for numerical calculations by using Eq. (7), where A (Si) and B (SiO$_2$) stacks, the materials with refractive indexes of $n_1 = 3.42$ (Si) and $n_2 = 1.52$ (SiO$_2$), and substrate $n_{sub} = 1.52$ (SiO$_2$) have been chosen [24]. The refractive indexes of both materials have been taken as constant. All regions have been thought of as linear and lossless. The outside medium has been assumed to be air and the layers have been assumed as dielectric. The layer thicknesses have been taken as $d_1 = 38.9\,nm$ and $d_2 = 87.5\,nm$ by using the quarter-wave equation $n_1d_1 = n_2d_2 = \lambda_0/4$, where $\lambda_0 = 532\,nm$ is the central wavelength. The number of periods N has been assumed as 24. All layers have been adjusted as quarter wavelengths. $\lambda_0 = 532\,nm$ represents the peak value of the sun's emission spectrum. Also,

it is important to investigate the properties of a perfect PC reflector for different wavelengths over the visible spectrum, as it will presumably be used in photovoltaic cells. This device for utilization must have a suitable reflectivity for a broad range of wavelength.

Figure 3 shows the reflectivity spectra, which have been maximized for $0°$, $30°$, $60°$, and $80°$ in TE polarization. With the increase of angles of the incidence, the maximum reflectance range increases.
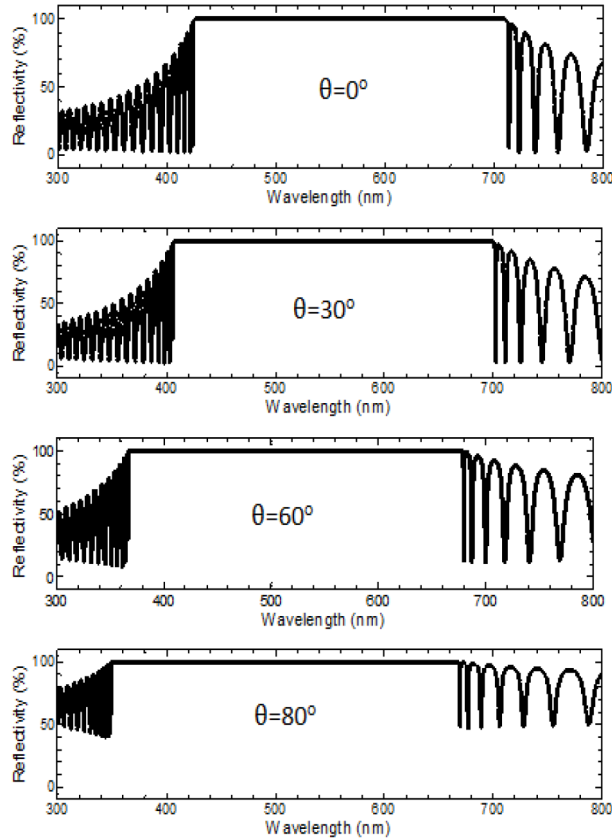

Figure 3. Reflectivity spectra of air/(AB)[24]/substrate and the different angles of incidence for TE polarization.

It is seen in Table 1 that there is just a small increase of $320 - 287 = 33$ nm in the bandwidth depending on the angle of incidence between $0°$ and $80°$. This is approximately equivalent to a rate of 11%. The band gap shifts a bit to the short wavelength range. Central wavelength λ_c equals 568 nm while the angle of incidence is $0°$. However, central wavelength λ_c reaches 509 nm by shifting through the short wavelength when the angle of incidence is $80°$. While designing the reflector to be used in PV cells, attention should be paid to the application between $0°$ and $80°$ since the maximum reflectance occurs for high incoming angles. Furthermore, by increasing the number of periods, far more outstanding reflectivity spectra can be achieved.

In Figure 4, the reflectivity spectrum is shown for the incidence angles of $0°$, $30°$, $60°$, and $80°$ in TM polarization. For the bandwidth where 100% reflectivity has occurred and the incidence angle has increased, it has been found that there is a certain increase of $287 - 172 = 115$ nm in the bandwidth in contrast to the state of TE polarization (Table 2).

The rate of increase equals approximately 40%. The bandwidth where 100% reflectivity has occurred is quite less than the state of TE polarization and has shifted through the region of short wavelength. Central wavelength λ_c equals 568 nm while the angle of incidence is $0°$.

Table 1. Reflection ranges for perfect PC in TE polarization.

Angle of incidence (degrees)	TE polarization Range of 100% reflectivity (nm)	Bandwidth (nm)	λ_c (nm)
0	425–712	287	568
30	406–700	294	553
60	367–678	311	522
80	349–669	320	509
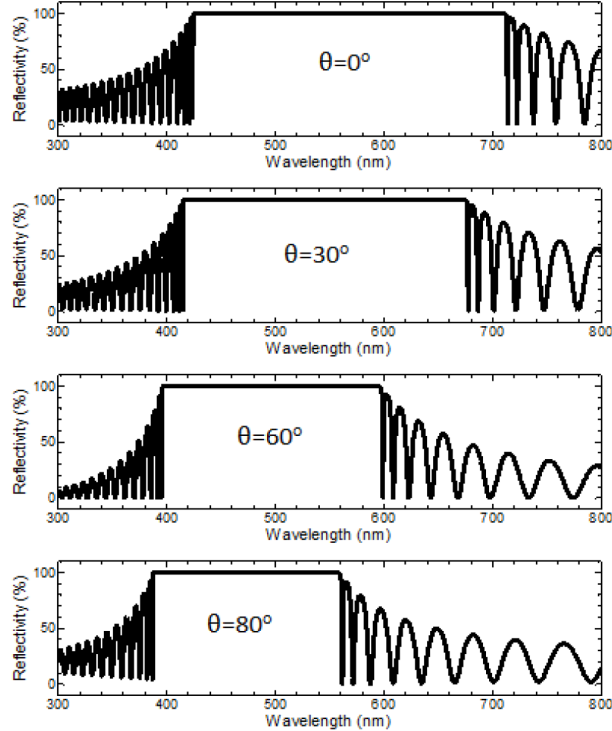
Figure 4. Reflectivity spectra of air/(AB)^{24}/substrate and the different angles of incidence for TM polarization.

Table 2. Reflection ranges for perfect PC in TM polarization.

Angle of incidence (degrees)	TE polarization Range of 100% reflectivity (nm)	Bandwidth (nm)	λ_c (nm)
0	425–712	287	568
30	415–675	260	545
60	396–597	201	496
80	387–559	172	473

However, the central wavelength λ_c reaches 473 nm by shifting through the short wavelength when the angle of incidence is $80°$.

As the bandwidth where the total 100% reflectivity has occurred in all the angles between $0°$ and $80°$ for TE mode is 244 nm, it is 134 nm for TM mode. Thus, the total bandwidth of the system is determined by TM mode. This case is important while designing the PV system.

4. Conclusion

We have presented the design and theoretical analysis of an optical broadband angular reflector for photovoltaic implementations based on a PC structure. We have obtained simulations of reflectivity spectra of this PC structure. By using 1D PC, a reflector with a wide bandwidth and operation in the visible range of the solar spectrum has been designed for a silicon solar cell. Bandwidth with a 100% reflectivity rate in the visible range has been obtained by analyzing the reflectivity spectrum for TE and TM modes. A wider bandwidth has been obtained in TE mode than TM mode. This designed structure can not only be used as a perfect back reflector in order to supply more absorption of the light within the solar cell concept, but can also be used as an angularly selective filter.

References

[1] Bermel, P.; Ghebrebrhan, M.; Chan, W.; Yeng, Y. X.; Araghchini, M.; Hamam, R.; Marton, C. H.; Jensen, K. F.; Soljacic, M.; Joannopoulos, J. D. et al. *Opt. Express* **2010**, *18*, A314-A334.

[2] Chen, J. Y.; Eric, L.; Chen, L. W. *Prog. Electromagn. Res.* **2011**, *17*, 1-11.

[3] Wang, W.; Hao, H. *Chin. Opt. Lett.* **2010**, *8*, 35-37.

[4] Mallick, S. B.; Agrawal, M.; Peumans, P. *Opt. Express* **2010**, *18*, 5691-5706.

[5] Liu, R.; Wu, Y.; Tong, G.; Xia, Z. *Chin. Opt. Lett.* **2013**, *11*, 134-136.

[6] Lee, H. Y.; Yao, T. *J. Appl. Phys.* **2003**, *93*, 819-830.

[7] Park, Y.; Drouard, E.; El Daif, O.; Letartre, X.; Viktorovitch, P.; Fave, A.; Kaminski, A.; Lemiti, M.; Seassal, C. *Opt. Express* **2009**, *17*, 14312-14321.

[8] Huang, X.; Han, S.; Huang, W.; Liu, X. *Chem. Soc. Rev.* **2013**, *42*, 173-201.

[9] Yablonovitch, E. *Phys. Rev. Lett.* **1987**, *58*, 2059-2062.

[10] John, S. *Phys. Rev. Lett.* **1987**, *58*, 2486-2489.

[11] Joannopoulos, J. D.; Meade, R. D.; Winn, J. N.; Johnson, S. G. *Photonic Crystals: Molding the Flow of Light*; Princeton University Press: Princeton, NJ, USA, 2008.

[12] Kirchartz, T. In *Physics of Nanostructured Solar Cells*; Badescu, V, Ed.; Nova Science Publishers: Hauppauge, NY, USA, 2009, pp. 1-40.

[13] Basore, P. A. *IEEE T. Electron. Dev.* **1990**, *37*, 337-343.

[14] Campbell, P. *Solar Energy Mater.* **1990**, *21*, 165-172.

[15] Battaglia, C.; Hsu, C. M.; Söderström, K.; Escarré, J.; Haug, F. J.; Charrière, M.; Boccard, M.; Despeisse, M.; Alexander, D. T. L.; Cantoni, M. et al. *ACS Nano* **2012**, *6*, 2790-2797.

[16] Kumar, V; Kumar, A; Singh, K. S.; Kumar, P. *Optoelectron. Adv. Mater.-Rapid Commun.* **2011**, *5*, 488-490.

[17] El Daif, O.; Drouard, E.; Gomard, G.; Kaminski, A.; Fave, A.; Lemiti, M.; Ahn, S.; Kim, S.; Cabarrocas, P. R.; Jeon, H. et al. *Opt. Express* **2010**, *18*, A293-A299.

[18] Buencuerpo, J.; Munioz-Camuniez, L. E.; Dotor, M. L.; Postigo, P. A. *Opt. Express* **2012**, *20*, A452-A464.

[19] Yu, Z.; Raman, A.; Fan, S. *Appl. Phys. A* **2011**, *105*, 329-339.

[20] Jiang, S.; Li, J.; Tang, J.; Wang, H. *Chin. Opt. Lett.* **2006**, *4*, 605-607.

[21] Kumar, V.; Singh, K.; Ojha S. P. *Optoelectron. Adv. Mater.-Rapid Commun.* **2010**, *4*, 19-22.

[22] Yariv, A.; Yeh, P. *Optical Waves in Crystals*; Wiley: New York, NY, USA, 1984.

[23] Born, M.; Wolf, E. *Principles of Optics*, 7th ed.; Cambridge University Press: Cambridge, UK, 2001.

[24] Weber, M. J. *Handbook of Optical Materials*; CRC Press: Boca Raton, FL, USA, 2003.